Preparation and evaluation of the PD0721-DOX antibody-drug conjugate targeting EGFRvIII to inhibit glioblastoma

MINMIN HU[1,2*], HONG LIU[1,2*], YUBING ZHANG[1], DINGYAN LU[3], LIN ZHENG[1], YONGLIN WANG[1], SHUAISHUAI CHEN[3] and TING LIU[1,2]

[1]State Key Laboratory of Functions and Applications of Medicinal Plants, Guizhou Provincial Key Laboratory of Pharmaceutics; [2]School of Pharmacy; [3]Engineering Research Center for The Development and Application of Ethnic Medicine and TCM (Ministry of Education)/National Engineering Research Center of Miao's Medicines, Guizhou Medical University, Guiyang, Guizhou 550004, P.R. China

Received September 16, 2023; Accepted March 6, 2024

DOI: 10.3892/etm.2024.12542

Abstract. Epidermal growth factor receptor variant III (EGFRvIII) is prominently expressed in various epithelial tumors. PD0721, a single-chain antibody (scFv), has been developed to specifically target EGFRvIII. Although doxorubicin (DOX) is an essential treatment approach for glioblastoma (GBM), its toxic effects and limited targeting capabilities are a challenge. To overcome the above limitations, antibody-drug conjugates (ADCs) have been developed to exploit the specificity of monoclonal antibodies in directing potent cytotoxic drugs to tumor cells expressing the target antigens. The present study aimed to conjugate DOX with PD0721 scFv to construct a PD0721-DOX ADC targeting EGFRvIII and examine its targeting effect and *in vitro* anti-GBM activity. PD0721-DOX ADC was generated by combining PD0721 scFv with DOX, using dextran T-10 as a linker. The drug-to-antibody ratio (DAR) was measured by ultraviolet and visible spectrophotometry (UV-Vis). A series of techniques, including cytotoxicity assays, immunofluorescence, cell internalization and flow cytometry assays were employed to evaluate the targeting efficacy and anti-GBM activity of the PD0721-DOX ADC. Following the conjugation of PD0721 scFv with DOX, the UV-Vis results showed a noticeable red shift in the maximum absorbance. The DAR of PD0721 scFv and DOX was 9.23:1. Cytotoxicity assays demonstrated that DK-MG cells treatment with PD0721-DOX ADC at 10 and 20 μg/ml significantly increased cytotoxicity compared with U-87MG ATCC cells (all $P<0.01$). Confocal microscopy revealed distinct green and red fluorescence in EGFRvIII-expressing DK-MG cells, while no fluorescence was observed in EGFRvIII negative U-87MG ATCC cells. Furthermore, compared with U-87MG ATCC cells, DK-MG cells showed effective internalization of the PD0721-DOX ADC ($P<0.001$). Finally, flow cytometric analyses indicated that the PD0721-DOX ADC significantly promoted the apoptosis of DK-MG cells compared with U-87MG ATCC cells ($P<0.01$). In summary, the current study suggested that the PD0721-DOX ADC could exhibit a notable targeting efficacy and potent anti-GBM activity.

Correspondence to: Dr Shuaishuai Chen, Engineering Research Center for The Development and Application of Ethnic Medicine and TCM (Ministry of Education)/National Engineering Research Center of Miao's Medicines, Guizhou Medical University, 9 Beijing Road, Yunyan, Guiyang, Guizhou 550004, P.R. China.
E-mail: sschen126@126.com

Dr Ting Liu, State Key Laboratory of Functions and Applications of Medicinal Plants, Guizhou Provincial Key Laboratory of Pharmaceutics, Guizhou Medical University, 9 Beijing Road, Yunyan, Guiyang, Guizhou 550004, P.R. China.
E-mail: liuting@gmc.edu.cn

[*]Contributed equally

Abbreviations: ADC, antibody-drug conjugate; DAR, drug-to-antibody ratio; Dex T-10, dextran T-10; DOX, doxorubicin; EGFR, epidermal growth factor receptor; EGFRvIII, epidermal growth factor receptor variant III; GBM, glioblastoma; IPTG, isopropyl β-D-thiogalactoside; scFv, single-chain antibody

Key words: antibody-drug conjugates, doxorubicin, single-chain antibodies, epidermal growth factor receptor variant III, glioblastoma

Introduction

Glioblastoma (GBM), a primary disease that severely endangers human health, is considered as a major disease that requires urgent global attention. GBM, as the most common prevalent primary malignant tumor, accounts for ~48% of all primary malignant tumors of the central nervous system and 57% of all gliomas (1,2). Chemotherapy is considered as the most common treatment strategy for malignant tumors (3). It has been reported that doxorubicin (DOX), an anthracycline antibiotic, can inhibit the growth of several solid tumors and hematological malignancies and it is considered as one of the most effective antitumor drugs currently available (4).

However, DOX has numerous disadvantages, including cardiotoxicity, liver toxicity and multidrug resistance (5-7). Therefore, the development of strategies that enhance targeting and minimize toxicity is of great importance for the clinical application of DOX.

Epidermal growth factor receptor (EGFR), an essential regulator of cellular growth in normal epithelial tissues, is a member of the cell surface receptor family, also known as human epidermal growth factor receptor 1 or ErbB1 (8,9). The members of the EGFR family play crucial roles in malignant cell transformation, drug resistance and metastasis of tumor stem cells and other tumor cells (10,11). For example, a previous study demonstrated that the signaling transduction of ErbB receptor tyrosine kinase could promote neuroblastoma growth (12). Notably, several mutations in the EGFR gene have been detected, with epidermal growth factor receptor variant III (EGFRvIII) being the most common one (13). Emerging evidence has suggested that EGFRvIII, a constitutively active mutant, can promote cell mitosis and support growth signaling, while it is involved in the development of several human epithelial malignancies (14). Other studies show that EGFRvIII was overexpressed in 80% of all human malignancies, including glioblastoma, lung cancer and gastric cancer, but not in normal tissues (15-19). Therefore, EGFRvIII could be a potential factor for the targeted therapy of GBM.

Antibody-drug conjugates (ADCs), which are novel antibody drugs, are composed of antibodies, cytotoxic drugs and their linkers (20). ADCs can precisely deliver potent cytotoxic drugs into malignant cells by binding to specific antigens on their surface (21). After internalization, ADCs are lysed, thus releasing cytotoxic drugs transferred by lysosomes to selectively kill tumor cells (22). It has been reported that ADCs can minimize the concentration of cytotoxic drugs in normal tissues and organs, while increasing their concentration in malignant tumors, eventually achieving high efficiency and low toxicity (23). Our research group had previously generated a single-chain antibody (scFv) using genetic engineering, called PD0721 scFv, which could target EGFRvIII (24,25). Specifically, the nucleic acid sequence of PD0721 scFv, targeting anti-EGFRvIII, was ligated with the pET-22b(+) plasmid to create the PD0721-pET recombinant plasmid, which was subsequently transformed into *Escherichia coli*. The monoclonal antibody was successfully obtained by inducing the mixture at an inducer concentration of 0.6 μM for 12 h at 15˚C until the OD600 of the bacterial solution reached ~0.6. The above findings could aid in the development of high-efficiency and low-toxicity ADCs targeting the EGFRvIII antigen.

In the present study, PD0721 scFv was conjugated with DOX to generate a PD0721-DOX ADC through an amine-aldehyde condensation reaction. The drug-to-antibody ratio (DAR) of PD0721 scFv and DOX was calculated by ultraviolet and visible spectrophotometry (UV-Vis). To evaluate the *in vitro* targeting efficacy and anti-GBM activity of the PD0721-DOX ADC, cytotoxicity assays, immunofluorescence, laser-scanning confocal microscopy and flow cytometric assays were performed. Given the difference between EGFRvIII-expressing DK-MG cells and U-87MG ATCC cells that do not express EGFRvIII (26,27), the present study aimed to investigate the targeting potential and cytotoxicity of PD0721-DOX ADC in the above two cell lines.

Materials and methods

Conjugation of PD0721 scFv with DOX. To obtain oxidized dextran T-10 (Dex T-10), 200 mg Dex T-10 was mixed with 2 ml of $NaIO_4$ (0.35 mmol/l, Xilong Chemical Co., Ltd.; cat no. 0408011), stirred in a flask at 150 rpm for 20 h in the dark, followed by freeze-drying. Subsequently, 10 mg DOX (Beijing Solarbio Science & Technology Co., Ltd.; cat no. D8740) was diluted into 2 ml ultrapure water and the mixture was then supplemented with 30 mg oxidized Dex T-10, followed by stirring at 150 rpm for 20 h in the dark. Then, to obtain the PD0721-DOX ADC, the oxidized Dex T-10/DOX mixture was supplemented with 5 mg PD0721 scFv, followed again by stirring at 150 rpm for 20 h at 4˚C in the dark. Subsequently, 100 μl $NaBH_4$ (0.13 mmol; Anhui Senrise Technology Co., Ltd.; cat no. EB180088) was added into the above mixture, which was then mixed at 150 rpm for 2 h at 37˚C in the dark. The final product was then subjected to ultrafiltration using a Millipore 10 k molecular weight ultrafiltration tube (MilliporeSigma).

Subsequently, the sample solution was added to a cuvette and through UV-Vis to obtain the UV absorption spectra (250-600 nm) and maximum absorption wavelength of Dex T-10, Oxidized Dex T-10, PD0721 scFv, DOX and PD0721-DOX ADCs, and compare the spectral differences.

DOX and PD0721 scFv concentration assessment. UV-Vis was employed to determine the concentration of PD0721 scFv and DOX. Therefore, 20 μg/ml DOX and 1 mg/ml bovine serum albumin (BSA; Beijing Solarbio Science & Technology Co., Ltd.; cat no. A8020) stock solutions were prepared in ultrapure water. The above stock solutions were used to prepare the DOX and PD0721 scFv standard solutions (0-20 μg/ml and 0-1 mg/ml, respectively) in ultrapure water. The concentration-absorbance standard curves of DOX and BSA were constructed by measuring their absorbance at wavelengths of 480, 280 and 280 nm, respectively. The above curves were utilized to determine the concentrations of PD0721 scFv and DOX in the PD0721-DOX ADC. The PD0721 scFv/DOX molar ratio was calculated using the following formula: DAR=(DOX concentration/DOX molar mass)/(PD0721 scFv concentration/PD0721 scFv molar mass).

Cell culture. DK-MG cells were purchased from the Otwo Biotech (Shenzhen) Inc. (cat no. HTX3018). U-87MG ATCC cells (glioblastoma of unknown origin) were purchased from the Procell Life Science & Technology Co., Ltd. (cat no. CL-0238). To verify the identity of U-87MG ATCC cells, short tandem repeat profiling was performed (PC-H2023072421). The cells were cultured in DMEM supplemented with 10% fetal bovine serum (Thermo Fisher Scientific Inc.; cat no. 10099-141C) at 37˚C in a 5% CO_2 environment. Experiments were performed using cells grown for four passages.

Cytotoxicity assay. DK-MG and U-87MG ATCC cells were seeded into 96-well plates at a density of $1.5x10^5$ cells/well and cultured to the logarithmic growth phase. PD0721-DOX ADC, DOX and PD0721 scFv were lyophilized to produce a powder, weighed using an electronic balance at a precision of 1:100,000 and dissolved in PBS to achieve the corresponding concentration. Subsequently, cells were treated with PD0721-DOX

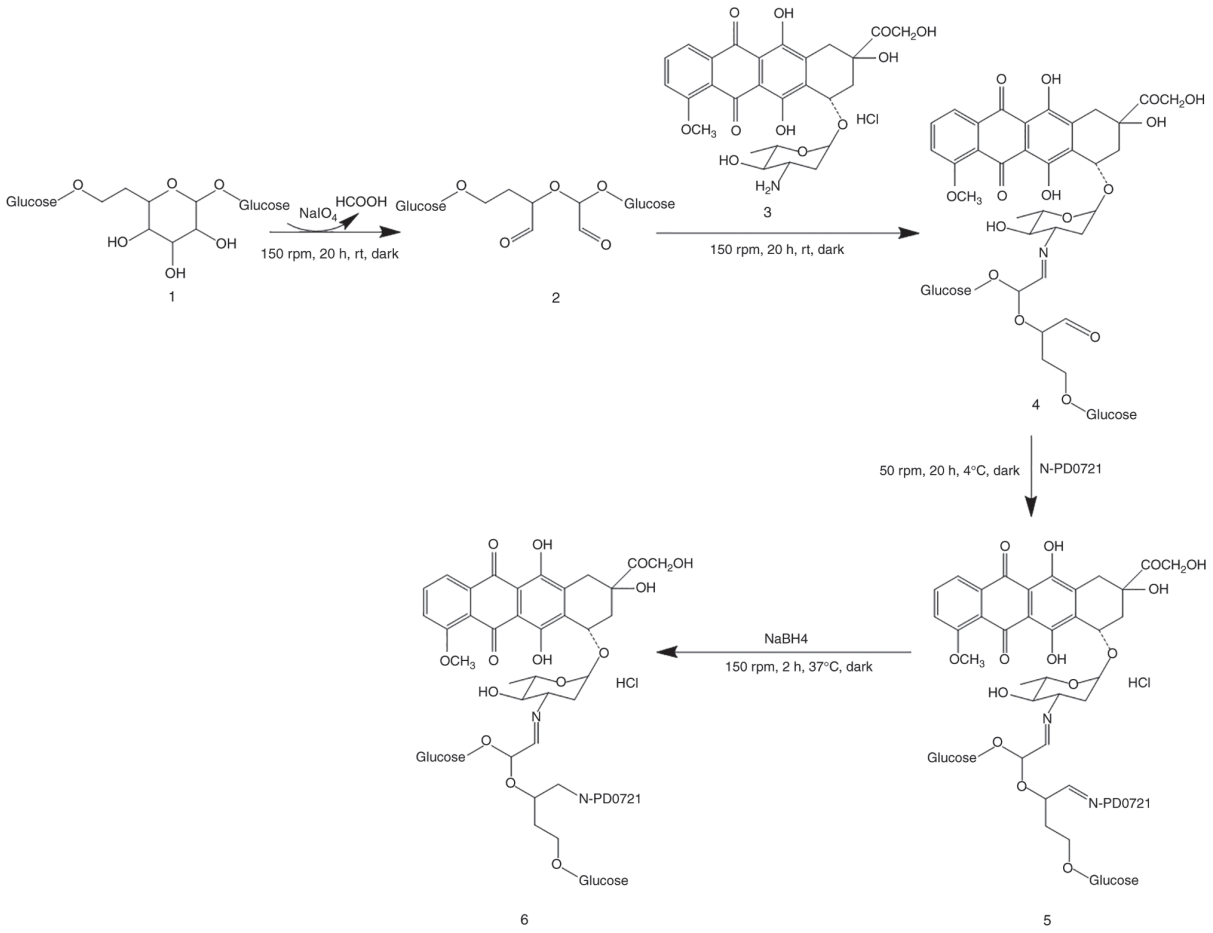

Figure 1. Design and synthesis of PD0721-doxorubicin antibody-drug conjugate. DOX:doxorubicin; ADC:antibody-drug conjugate; rt, room temperature.

ADC, DOX, or PD0721 scFv at varying concentrations (0, 5, 10 and 20 μg/ml). Following incubation for 24 h, cell viability was assessed using a Cell Counting Kit-8 assay (Dojindo Laboratories, Inc.; cat no. CK04).

Immunofluorescence staining. DK-MG and U-87MG ATCC cells were seeded onto glass coverslips at a density of 1.0×10^5 cells/coverslip. Following attachment, cells were treated with 20 μg/ml PD0721 scFv or PD0721-DOX ADC for 2 h. Subsequently, cells were fixed with 4% paraformaldehyde (Absin Bioscience Inc.; cat no. abs9179) for 15 min in room temperature, followed by permeabilization with 0.1% Triton X-100 (Beijing Solarbio Science & Technology Co., Ltd.; cat no. T8200) for 15 min. The cells were then incubated with 2% BSA (Beijing Solarbio Science & Technology Co., Ltd.; cat no. A8020) at 37˚C for 30 min, followed by incubation with FITC-H&L labelled goat anti-human IgG (Abcam; cat no. ab6854) in the dark at 37˚C for 1 h and DAPI (1:500; Absin Bioscience Inc.; cat no. abs47047616) for 5 min in room temperature. The cells were observed and images were captured with confocal laser microscope (x630 magnification; ZEN system software 3.0; Zeiss AG) and analyzed region-wide.

Process of drug entry into cells. DK-MG and U-87MG ATCC cells were seeded on glass coverslips at a density of 1.0×10^5 cells/coverslip. Upon attachment, cells were treated with 20 μg/ml PD0721-DOX ADC or DOX incubated for 1, 3 and 6 h. Subsequently, the cells were observed and images were captured using confocal laser microscope (x200 magnification; ZEN system software 3.0; Zeiss AG) and analyzed region-wide.

Flow cytometry. DK-MG and U-87MG ATCC cells were seeded into 6-well plates at a density of 5.0×10^5 cells/well. After reaching logarithmic-growth phase, cells were treated with 20 μg/ml PD0721-DOX ADC, DOX, or PD0721 scFv for 24 h. Subsequently, to distinguish between alive and dead cells, the cells were stained with Annexin V-APC and 7-ADD (Annexin V-APC/7-AAD Apoptosis Analysis Kit, Absin Bioscience Inc., cat no. abs50008) for 10 and 5 min, respectively, at room temperature and away from light. Finally, cell apoptosis was analyzed using a BD Accuri C6 Plus flow cytometer (BD Biosciences) and the data were assessed using FlowJo 10.6 software (FlowJo LLC). Apoptotic rate was calculated as the percentage of early + late apoptotic cells relative to the control.

Statistical analysis. Data analysis was performed using SPSS 26.0 software (IBM Corp.) and GraphPad Prism 8 software (GraphPad; Dotmatics). The results are expressed as the mean ± standard deviation and are representative of three independent experiments. Differences between two groups were analyzed using Student's t-test and correlation analysis was performed using Pearson's correlation analysis. $P<0.05$ was considered to indicate a statistically significant difference.

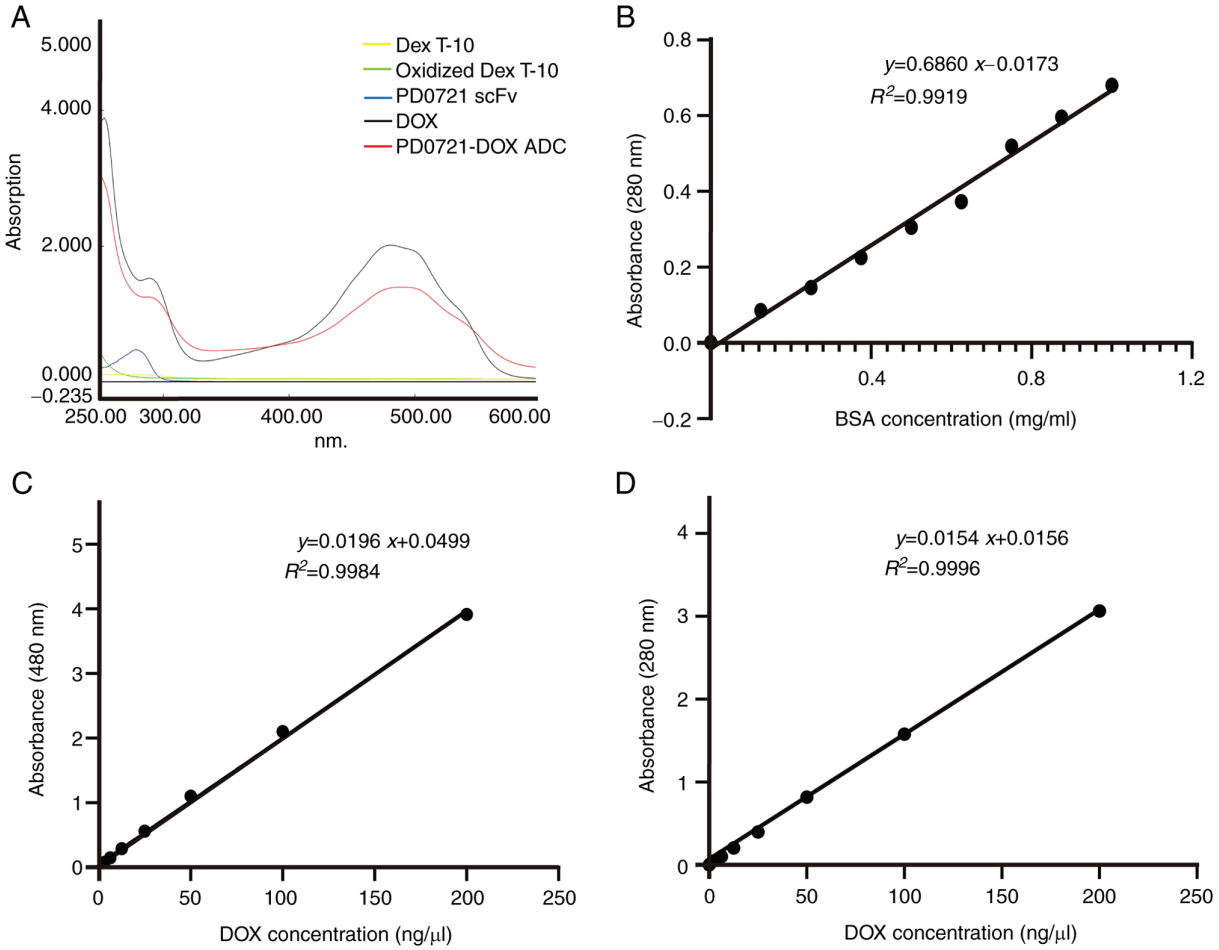

Figure 2. UV-Vis absorption spectra. (A) UV-Vis absorption is shown. Standard curves of (B) PD0721 scFv (280 nm), (C) DOX (480 nm) and (D) DOX (280 nm). UV-Vis, ultraviolet and visible spectrophotometry; DOX, doxorubicin; ADC, antibody-drug conjugate; Dex T-10, dextran T-10; scFv, single-chain antibody.

Results

Conjugation of PD0721 scFv with DOX. Strategies based on ADC design were applied to enhance DOX targeting. Therefore, compound 1 was oxidized to form linker 2 containing dialdehyde. The two aldehyde groups of linkers 2 were connected to DOX and N-PD0721. First, the amino group of DOX and the aldehyde group of linker 2 underwent an additional reaction followed by dehydration to form a carbon nitrogen bond, eventually obtaining DOX derivative 4. In addition, the aldehyde group of DOX derivative 4 underwent the same reactions as N-PD07121 to obtain compound 5. Finally, the target compound 6 was obtained by reducing compound 5 with $NaBH_4$ (Fig. 1).

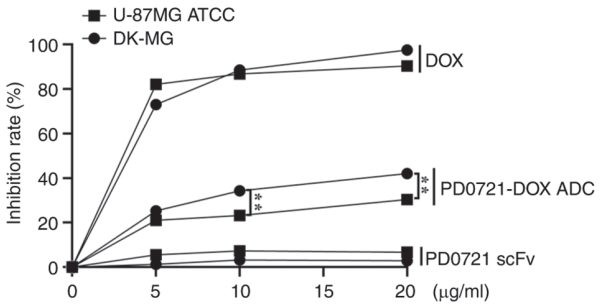

Figure 3. DOX, PD0721-DOX ADC and PD0721 scFv induced cytotoxicity in DK-MG and U-87MG ATCC cells. **P<0.01. DOX, doxorubicin; ADC, antibody-drug conjugate; scFv, single-chain antibody.

UV-Vis-mediated identification of PD0721-DOX ADC and DAR of PD0721 scFv/DOX. The maximum absorbance of DOX was ~470 nm, while that following DOX conjugation with PD0721 scFv (red shifted) was ~490 nm, thus indicating that PD0721 scFv and DOX were successfully conjugated (Fig. 2A). Subsequently, the PD0721 scFv and DOX standard curves at 280 and 480 nm were drawn (Fig. 2B and C). The absorbance of PD0721-DOX ADC at a wavelength of 480 nm was inserted into the regression equation of DOX standard curve. Therefore, the analysis revealed that DOX concentration in the PD0721-DOX ADC was 2.7 mg/ml. Since DOX also shows interference absorption at 280 nm, the standard curve of DOX at 280 nm was also plotted. Therefore, the regression equation of the DOX standard curve was obtained at 280 nm (Fig. 2D). Based on the DOX concentration of 2.7 mg/ml, the interference absorbance of DOX at a wavelength of 280 nm was 1.06. After subtracting the interference absorbance of DOX at 280 nm from that of PD0721-DOX ADC at 280 nm, the resulting value was then entered into the PD0721 scFv standard curve regression

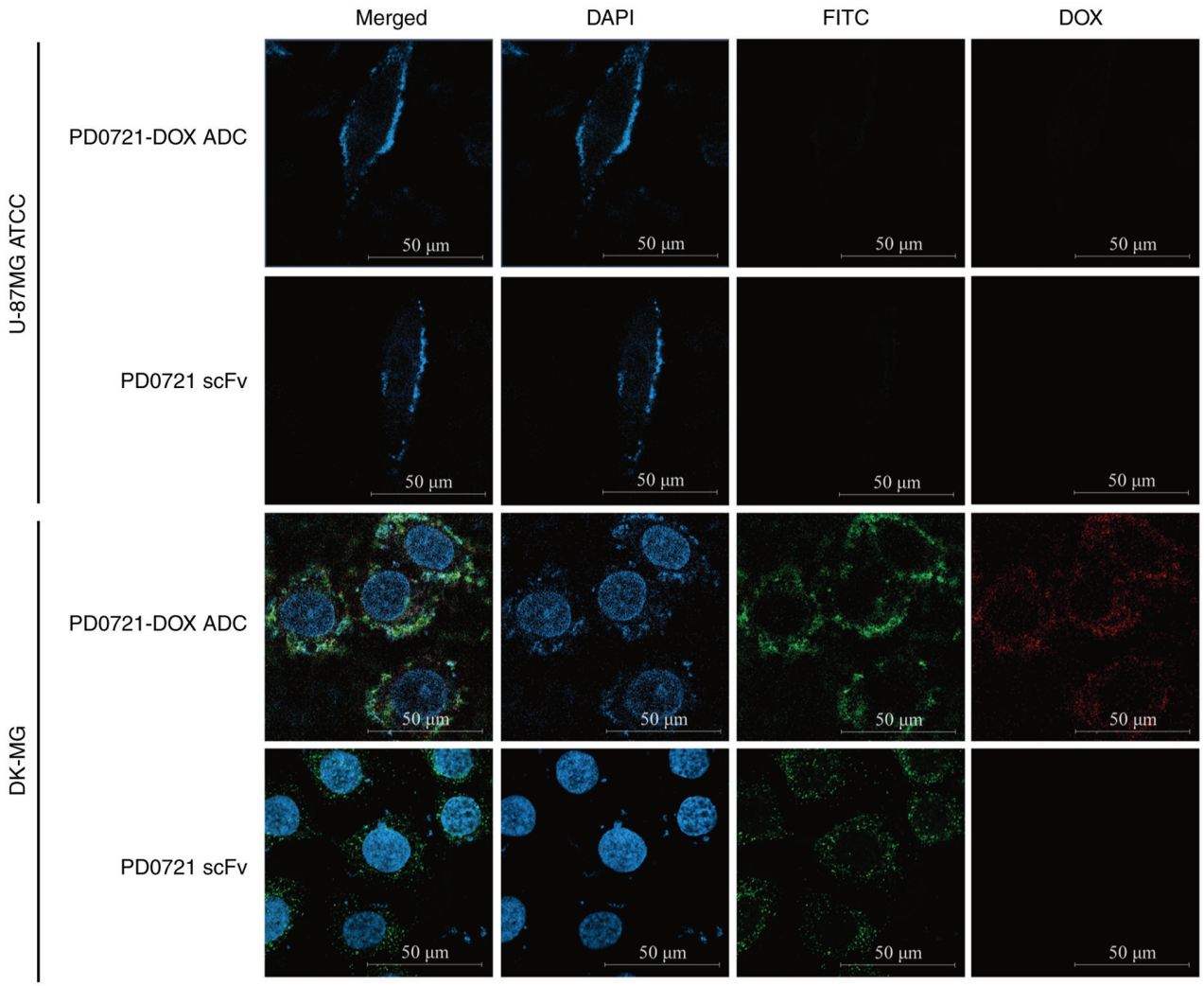

Figure 4. Representative confocal images of the PD0721-DOX ADC and PD0721 scFv in DK-MG and U-87MG ATCC cells. Blue luminescence indicates cell nuclei, while green and red luminescence indicate PD0712 scFv and DOX, respectively (scale bars, 50 μm). DOX, doxorubicin; ADC, antibody-drug conjugate; scFv, single-chain antibody.

equation. Therefore, the concentration of PD0721 scFv in PD0721-DOX ADC was estimated at 13.2 mg/ml. Based on the concentration-absorbance standard curve, the DAR of PD0721 scFv and DOX was calculated to be 9.23:1, thus indicating that each PD0721 scFv molecule was conjugated with ~9.23 DOX molecules.

PD0721-DOX ADC promotes cytotoxicity in DK-MG cells. To further validate the anti-GBM efficacy of PD0721-DOX ADC, its effects on cytotoxicity of DK-MG and U-87MG ATCC cells were investigated. PD0721-DOX ADC at 10 and 20 μg/ml significantly inhibited DK-MG cell proliferation compared with U-87MG ATCC cells (all P<0.01; Fig. 3). However, cells treatment with PD0721 scFv or DOX alone did not exhibit significant differences in DK-MG and U-87MG ATCC cell proliferation, thus indicating that the developed PD0721-DOX ADC possessed particular targeting activity, while maintaining toxicity. Therefore, in subsequent experiments, the most effective dosage identified in the preliminary studies was used, a 20-μg/ml concentration of PD0721-DOX ADC, to ensure the most optimal experimental conditions were achieved.

PD0721-DOX ADC can specifically target EGFRvIII. Microscopic analysis demonstrated that EGFRvIII-expressing DK-MG cells treated with PD0721 scFv or PD0721-DOX ADC emitted strong green fluorescence compared with the U-87MG ATCC cells (not expressing EGFRvIII), thus verifying the high specificity of PD0721 scFv for targeting EGFRvIII (Fig. 4). Additionally, prominent red fluorescence was observed in DK-MG cells after treatment with PD0721-DOX ADC, thus providing additional evidence of the successful construction of the PD0721-DOX ADC.

PD0721-DOX ADC is well internalized by DK-MG cells. Microscopic observation revealed an increase in red fluorescence in the U-87MG ATCC cell lines compared with that in the DK-MG cells after DOX treatment (all P<0.01; Fig. 5A and B). However, a significant red fluorescence was observed in DK-MG cells compared with U-87MG ATCC cells following treatment with PD0721-DOX ADC, especially at 1, 3 and 6 h after treatment (all P<0.001; Fig. 5A and C), highlighting the excellent specificity of PD0721-DOX ADC.

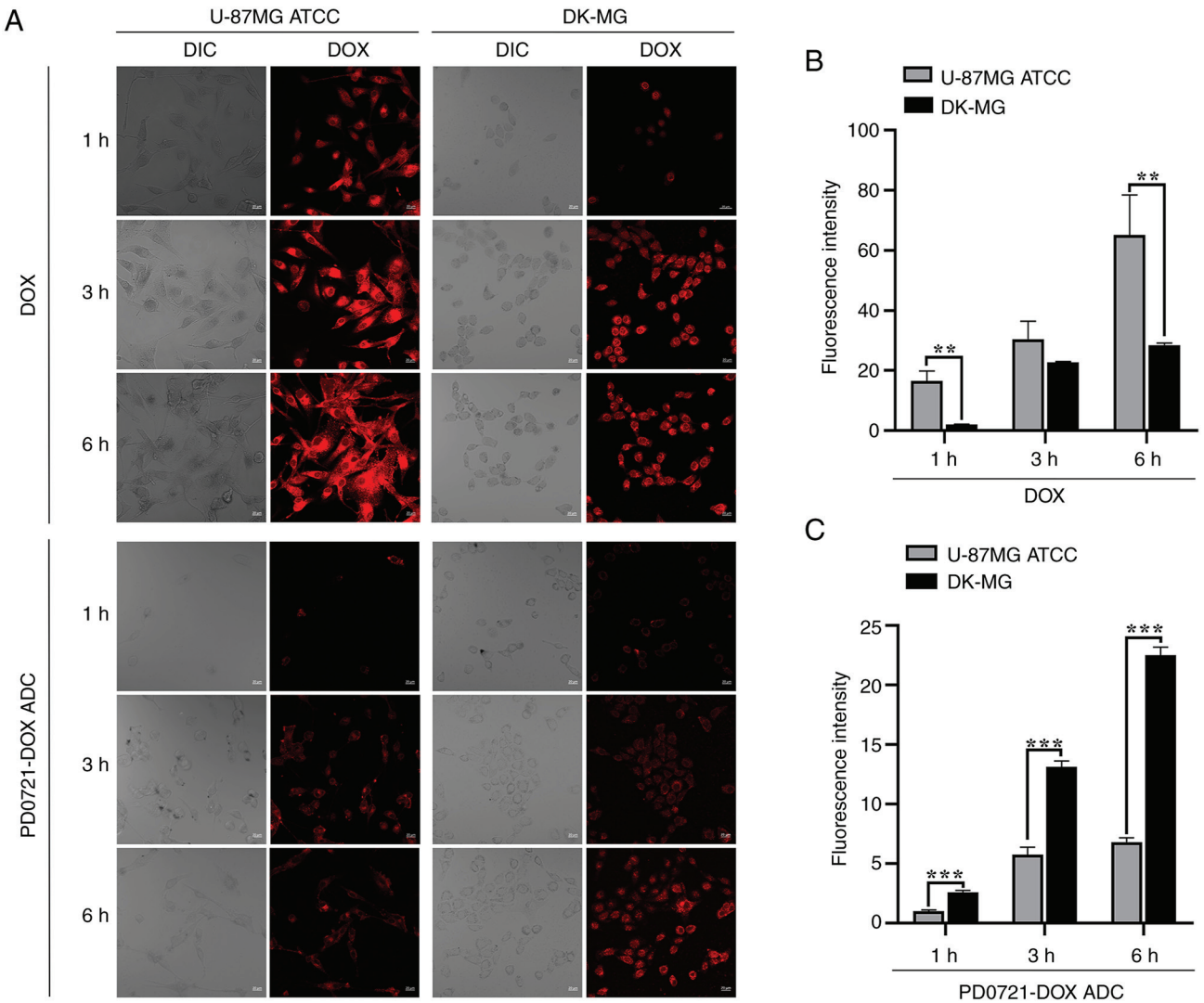

Figure 5. Internalization assessment of DOX and PD0721-DOX ADC in two types of cells. (A) Representative confocal images and fluorescence intensity of (B) DOX and (C) PD0721-DOX ADC in DK-MG and U-87MG ATCC cells. Bright field indicates cells and red luminescence indicates DOX (scale bars, 20 μm). **P<0.01 and ***P<0.001. DOX, doxorubicin; ADC, antibody-drug conjugate.

PD0721-DOX ADC promotes apoptosis in DK-MG cells. The effect of PD0721-DOX ADC on inducing cell apoptosis was further evaluated by flow cytometry. The results showed that cell treatment with PD0721 scFv and DOX alone could not cause significant differences between DK-MG and U-87MG ATCC cells. However, PD0721-DOX ADC notably promoted the apoptosis of DK-MG cells compared with U-87MG ATCC cells (P<0.01; Fig. 6), thus suggesting that PD0721-DOX ADC could exert a strong anti-GBM activity. The aforementioned findings highlighted the targeting specificity of PD0721-DOX ADC towards EGFRvIII and its potential as an anti-GBM factor.

Discussion

Chemotherapeutic drugs commonly exhibit strong cytotoxicity against tumor cells. However, they can also cause damage to normal cells (28). ADCs have the potential to enhance the efficacy of chemotherapeutic drugs against tumor cells, while minimizing their toxicity on normal cells (23,29). The present study aimed to describe the construction of a PD0721-DOX ADC through the chemical coupling of PD0721 scFv with DOX. Furthermore, it aimed to investigate the targeting ability and apoptosis-inducing potential of PD0721-DOX ADC *in vitro* in DK-MG and U-87MG ATCC cells. The PD0721-DOX ADC was developed via using a chemical method to couple PD0721 scFv with DOX. The *in vitro* experiments verified that the PD0721-DOX ADC was efficiently internalized by GBM cells and exhibited excellent targeting ability towards EGFRvIII-expressing DK-MG cells. Furthermore, PD0721-DOX ADC could notably enhance cytotoxicity and apoptosis in DK-MG cells compared with U-87MG ATCC cells.

Given the crucial role of EGFRvIII in GBM, in a previous study of our laboratory, novel monoclonal antibodies were generated and their efficiency was compared with that of commercially available antibodies (24,25). Emerging evidence has suggested that dextran is a high-molecular polysaccharide compound formed by interconnecting glucose through 1,6-glycosidic bonds. Due to its non-toxicity, water solubility and good biocompatibility, dextran has been used extensively in the biomedical and pharmaceutical fields (30). Herein, Dex T-10 was utilized as a linker for the preparation of PD0721-DOX ADC. Following conjugation of PD0721 scFv with DOX, the

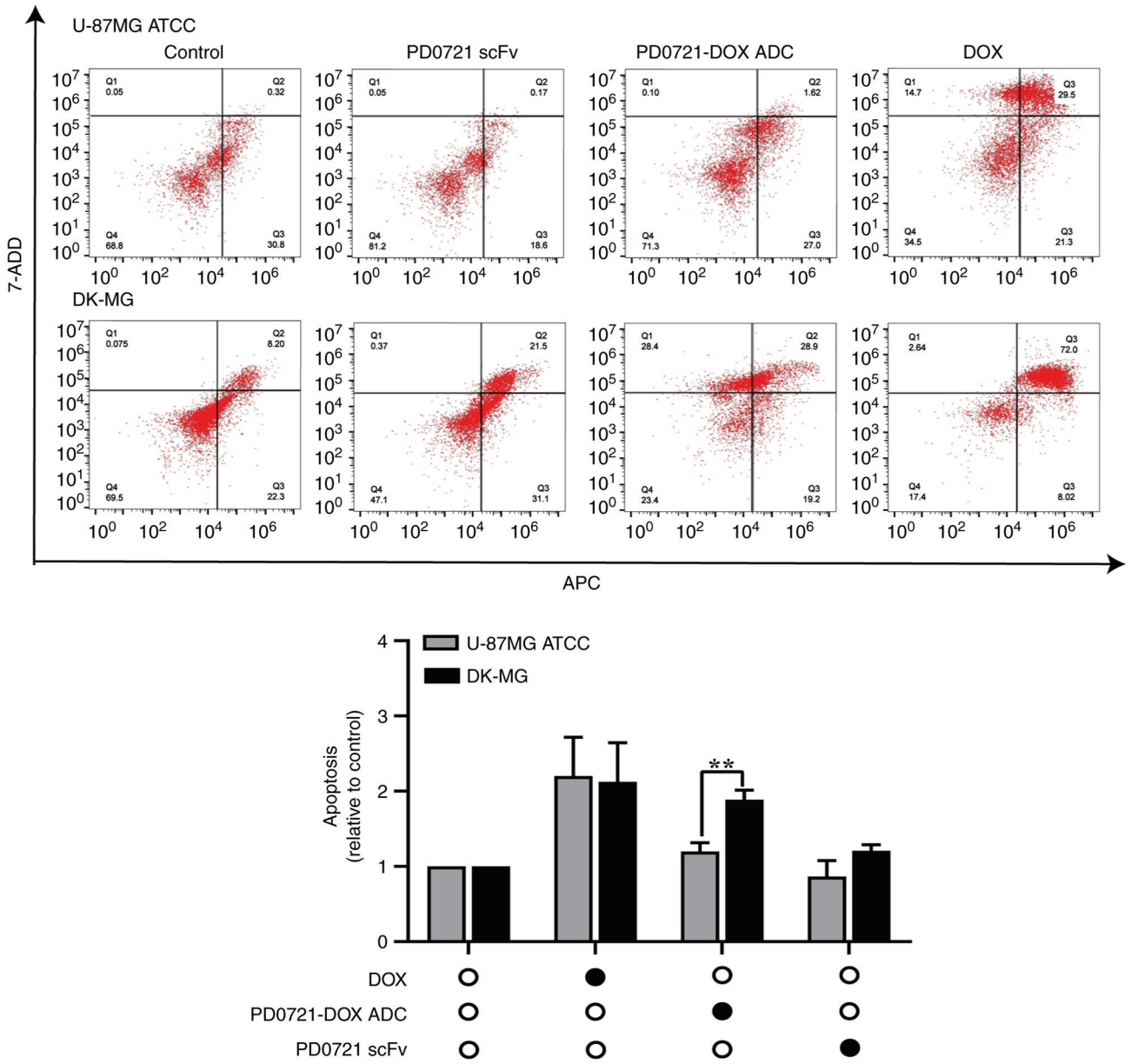

Figure 6. Evaluation of DOX, PD0721-DOX ADC and PD0721 scFv-induced apoptosis in DK-MG and U-87MG ATCC cells. **P<0.01. DOX, doxorubicin; ADC, antibody-drug conjugate; scFv, single-chain antibody.

UV-Vis spectrum analysis revealed a significant red shift in the maximum absorption, primarily attributed to the presence of two aldehyde groups in oxidized Dex T-10. The latter could undergo condensation with the amino groups in DOX and PD0721 scFv, thus forming a covalent cross-linking structure, known as the Schiff base (31). As a result, the molecular weight and the degree of conjugation were increased. Therefore, the UV-Vis absorption displayed a pronounced red-shift. The aforementioned results verified the successful coupling of PD0721 scFv with DOX. Based on UV-Vis, the DAR of PD0721 scFv and DOX was estimated to be 9.23:1.

In establishing the dosage parameters for the experiments, the present study initially conducted a series of preliminary tests to ascertain the effective dose range of the PD0721-DOX ADC. Acknowledging the complexities involved in preparing PD0721-DOX ADC samples, a concentration range was carefully selected, specifically 0, 5, 10 and 20 μg/ml, for thorough investigation. Furthermore, in determining the optimal treatment duration, the preliminary experiments revealed that the PD0721-DOX ADC antibody gradually exhibited increased cytotoxicity over time. Consequently, a different treatment period in was chosen for experiments to more effectively demonstrate the cytotoxic efficacy of PD0721-DOX ADC against cancer cells. CCK-8 assays were carried out to assess the cytotoxicity effect of PD0721-DOX ADC on GBM cell lines. Therefore, PD0721-DOX ADC significantly inhibited the proliferation of DK-MG cells compared with U-87MG ATCC cells, thus indicating a particular cytotoxic effect of PD0721-DOX ADC on DK-MG cells.

The mechanism of action of ADC includes two main processes, namely its specifically binding to the target and subsequent internalization of the antibody drugs (32). Following internalization, ADCs are transported intracellularly from the early to the late endosome and eventually reach

the lysosomal compartment, where the cytotoxic payload is released to promote cell death. (22) In the present study, the immunofluorescence results detected green (PD0721 scFv) and red fluorescence (DOX) on the surface of DK-MG cells. By contrast, due to the absence of the EGFRvIII antigen on their surface, U-87MG ATCC cells did not exhibit noticeable green or red fluorescence, thus indicating that PD0721-DOX ADC could directly target EGFRvIII-expressing cells. Further, the cell internalization results demonstrated superior and faster entry of PD0721-DOX ADC into DK-MG cells, compared with U-87MG ATCC cells. To minimize experimental errors, an Annexin V-APC/7-AAD apoptosis detection kit was utilized to detect apoptosis in PD0721-DOX ADC-treated cancer cells. The results demonstrated that PD0721-DOX ADC effectively induced DK-MG cell apoptosis, thus supporting its potent anti-GBM activity. Furthermore, the variations in DOX levels between the two cell types may be attributed to various factors, such as cell type distinctions and drug transporters, which will be the focus of further comprehensive examination and analysis.

However, the present study had some limitations. Firstly, *in vivo* experiments and *in vitro* (co-cultivation of DK-MG and U-87MG ATCC cells) should be performed to validate the findings of the current study and provide additional insights beyond the current *in vitro* verification. Although co-culture of the two types of cells was attempted, difficulties were encountered in distinguishing them under the microscope. Despite these challenges there will be further exploration of strategies and methodologies employed in the co-culturing of the two cell types. Second, the experimental conditions should be further optimized to enhance the targeting specificity and anti-GBM effect of PD0721-DOX ADC in DK-MG cells. However, PD0721-DOX ADC could offer a novel therapeutic approach for malignant tumors and lays a foundation for the clinical application of DOX.

In summary, in the present study a PD0721-DOX ADC delivery system was constructed through conjugating PD0721 scFv with DOX using Dex T-10 to enhance the targeting capacity of DOX against EGFRvIII. The results demonstrated that PD0721-DOX ADC exhibited effective targeting against the EGFRvIII antigen, while it could significantly promote cytotoxicity and cell apoptosis. The findings hold potential implications for the advancement of ADC and DOX development and the treatment of GBM in clinical practice.

Acknowledgements

Not applicable.

Funding

The present study was supported by grants from the project of the National Natural Science Foundation of China (grant no. 82360817), Guizhou Science and Technology Department [grant nos. ZK(2022) key 037, (2021)5619 and (2023)006].

Availability of data and materials

The data generated in the present study may be requested from the corresponding author.

Authors' contributions

SC and TL conceived the present study. YZ and DL were responsible for designing the study and for data authentication. MH and HL were responsible for data analysis, writing and original draft preparation. LZ and YW were responsible for the assessment of all the raw data. SC and TL were responsible for project supervision and administration. LZ and TL were responsible for funding acquisition. MH and TL confirm the authenticity of all the raw data. All authors have read and approved the final manuscript.

Ethics approval and consent to participate

Not applicable.

Patient consent for publication

Not applicable.

Competing interests

The authors declare that they have no competing interests.

References

1. Tan AC, Ashley DM, López GY, Malinzak M, Friedman HS and Khasraw M: Management of glioblastoma: State of the art and future directions. CA Cancer J Clin 70: 299-312, 2020.
2. Sung H, Ferlay J, Siegel RL, Laversanne M, Soerjomataram I, Jemal A and Bray F: Global cancer statistics 2020: GLOBOCAN estimates of incidence and mortality worldwide for 36 cancers in 185 countries. CA Cancer J Clin 71: 209-249, 2021.
3. Avazzadeh R, Vasheghani-Farahani E, Soleimani M, Amanpour S and Sadeghi M: Synthesis and application of magnetite dextran-spermine nanoparticles in breast cancer hyperthermia. Prog Biomater 6: 75-84, 2017.
4. Tang L, Jiang WH, Wu L, Yu XL, He Z, Shan WG, Fu LL, Zhang ZH and Zhao YC: TPGS2000-DOX prodrug micelles for improving breast cancer therapy. Int J Nanomedicine 16: 7875-7890, 2021.
5. Yang N, Ma HY, Jiang Z, Niu LH, Zhang XS, Liu YY, Wang YH, Cheng ST, Deng Y, Qi HY and Wang ZR: Dosing depending on SIRT3 activity attenuates doxorubicin-induced cardiotoxicity via elevated tolerance against mitochondrial dysfunction and oxidative stress. Biochem Biophys Res Commun 517: 111-117, 2019.
6. Aljobaily N, Viereckl MJ, Hydock DS, Aljobaily H, Wu TY, Busekrus R, Jones B, Alberson J and Han Y: Creatine alleviates doxorubicin-induced liver damage by inhibiting liver fibrosis, inflammation, oxidative stress and cellular senescence. Nutrients 13: 41, 2020.
7. Guo Y, Ding YY, Zhang T and An HL: Sinapine reverses multi-drug resistance in MCF-7/dox cancer cells by down-regulating FGFR4/FRS2α-ERK1/2 pathway-mediated NF-κB activation. Phytomedicine 23: 267-273, 2016.
8. Santos EDS, Nogueira KAB, Fernandes LCC, Martins JRP, Reis AVF, Neto JBV, Júnior I, Pessoa C, Petrilli R and Eloy JO: EGFR targeting for cancer therapy: Pharmacology and immunoconjugates with drugs and nanoparticles. Int J Pharm 592: 120082, 2021.
9. Li MF, Yang JL, Zhang LH, Tu SF, Zhou X, Tan Z, Zhou WJ, He YJ and Li YH: A low-molecular-weight compound exerts anticancer activity against breast and lung cancers by disrupting EGFR/Eps8 complex formation. J Exp Clin Cancer Res 38: 211, 2019.
10. Sigismund S, Avanzato D and Lanzetti L: Emerging functions of the EGFR in cancer. Mol Oncol 12: 3-20, 2018.
11. Hampton KK and Craven RJ: Pathways driving the endocytosis of mutant and wild-type EGFR in cancer. Oncoscience 1: 504-512, 2014.

12. Richards KN, Zweidler-McKay PA, Van Roy N, Speleman F, Trevino J, Zage PE and Hughes DP: Signaling of ERBB receptor tyrosine kinases promotes neuroblastoma growth in vitro and in vivo. Cancer 116: 3233-3243, 2010.
13. Gan HK, Cvrljevic AN and Johns TG: The epidermal growth factor receptor variant III (EGFRvIII): Where wild things are altered. FEBS J 280: 5350-5370, 2013.
14. Guo G, Gong K, Wohlfeld B, Hatanpaa KJ, Zhao D and Habib AA: Ligand-independent EGFR signaling. Cancer Res 75: 3436-3441, 2015.
15. Zheng Y, Ma Y, Yue H, Liu GZ and Han SY: EGFRvIII epigenetically regulates ARHI to promote glioma cell proliferation and migration. Exp Mol Pathol 112: 104344, 2020.
16. Yang K, Ren X, Tao L, Wang P, Jiang H, Shen L, Zhao Y, Cui Y, Li M and Lin S: Prognostic implications of epidermal growth factor receptor variant III expression and nuclear translocation in Chinese human gliomas. Chin J Cancer Res 31: 188-202, 2019.
17. Zhang Z, Jiang J, Wu X, Zhang M, Luo D, Zhang R, Li S, He Y, Bian H and Chen Z: Chimeric antigen receptor T cell targeting EGFRvIII for metastatic lung cancer therapy. Front Med 13: 57-68, 2019.
18. Bagley SJ and O'Rourke DM: Clinical investigation of CAR T cells for solid tumors: Lessons learned and future directions. Pharmacol Ther 205: 107419, 2020.
19. Wee P and Wang Z: Epidermal growth factor receptor cell proliferation signaling pathways. Cancers 9: 52, 2017.
20. Nagayama A, Ellisen LW, Chabner B and Bardia A: Antibody-drug conjugates for the treatment of solid tumors: Clinical experience and latest developments. Target Oncol 12: 719-739, 2017.
21. Sievers EL and Senter PD: Antibody-drug conjugates in cancer therapy. Annu Rev Med 64: 15-29, 2013.
22. Okajima D, Yasuda S, Maejima T, Karibe T, Sakurai K, Aida T, Toki T, Yamaguchi J, Kitamura M, Kamei R, *et al*: Datopotamab deruxtecan, a novel TROP2-directed antibody-drug conjugate, demonstrates potent antitumor activity by efficient drug delivery to tumor cells. Mol Cancer Ther 20: 2329-2340, 2021.
23. Hafeez U, Parakh S, Gan HK and Scott AM: Antibody-drug conjugates for cancer therapy. Molecules 25: 4764, 2020.
24. Zhang YB, Wu ZX, He B, Yang C, Li YJ and Liu T: Establishment and optimization of an ELISA for affinity detection of single-chain antibodies to EGFRvIII. Xi Bao Yu Fen Zi Mian Yi Xue Za Zhi 37: 73-78, 2021 (In Chinese).
25. Zhang YB, Ye LF, Wu ZX, Xue WN, He B, Yang C, Li YJ, Wang YL and Liu T: Optimization and identification of prokaryotic expression conditions of PD0721 single-chain antibody in vitro. J Food Sci Biotech 40: 42-49, 2021.
26. Struve N, Riedel M, Schulte A, Rieckmann T, Grob TJ, Gal A, Rothkamm K, Lamszus K, Petersen C, Dikomey E and Kriegs M: EGFRvIII does not affect radiosensitivity with or without gefitinib treatment in glioblastoma cells. Oncotarget 6: 33867-33877, 2015.
27. Allen M, Bjerke M, Edlund H, Nelander S and Westermark B: Origin of the U87MG glioma cell line: Good news and bad news. Sci Transl Med 8: 354re3, 2016.
28. Zraik IM and Heß-Busch Y: Management of chemotherapy side effects and their long-term sequelae. Urologe A 60: 862-871, 2021 (In German).
29. Fu ZW, Li SJ, Han SF, Shi C and Zhang Y: Antibody drug conjugate: The 'biological missile' for targeted cancer therapy. Signal Transduct Target Ther 7: 93, 2022.
30. Hu QB, Lu YJ and Luo YC: Recent advances in dextran-based drug delivery systems: From fabrication strategies to applications. Carbohydr Polym 264: 117999, 2021.
31. Helal MH, Al-Mudaris ZA, Al-Douh MH, Osman H, Wahab HA, Alnajjar BO, Abdallah HH and Abdul Majid AM: Diaminobenzene schiff base, a novel class of DNA minor groove binder. Int J Oncol 41: 504-510 2012.
32. Marei HE, Cenciarelli C and Hasan A: Potential of antibody-drug conjugates (ADCs) for cancer therapy. Cancer Cell Int 22: 255, 2022.